J. Bamboo and Rattan, Vol. 3, No. 2, pp. 107–121 (2004)

Bamboo-precocious wood composite beams: theoretical prediction of the bending behaviour

YOSHIAKI AMINO *

Laboratory of Timber Construction, IBOIS, Swiss Federal Institute of Technology Lausanne, CH-1015 Lausanne, Switzerland

Abstract—A type of sandwich beam, consisting of thin bamboo facings and poplar core, is proposed by the author, in order to increase the use of abundant precocious woods by reinforcing with bamboo layers. The objectives of this study are the experimental characterization of the static bending behaviour of the proposed sandwich beam and examining the theoretical predictability of the behaviour. The moment–deflection curve, computed on the basis of the stress extension across the beam section, corresponded remarkably well to the actual curves from the experiments. This computation method, interpreting the mechanical contribution of the thin bamboo facings to the bending capacity improvement, can be considered effective to estimate the ultimate strength, as well as the elastic plastic deflection evolution of the sandwich beam.

Key words: Composite; sandwich beam; precocious wood; poplar; reinforcement; bending behaviour; ultimate strength; theoretical estimation.

INTRODUCTION

Precocious species, like poplar, often show a mechanical performance being insufficient for building structure. They are rarely used as building material, and thence their commercial value is consequently much lower than the conifers from industrialized plantation. Such partiality of commercial value can be considered one of the reasons for the forest destruction in warm regions covered with precocious woods. The conception of the bamboo-precocious wood composite beam was proposed by the author in order to develop the use of weak precocious woods by reinforcing with thin bamboo layers [1]. Despite the fact that bamboo, usually found in warm regions, is also precocious, it can provide high strength materials appropriate for the proposed reinforcement.

*E-mail: yoshiaki.amino@epfl.ch

Establishing design methods is indispensable for the application of these beams in actual buildings. This study was carried out so as to discuss the loading capacity prediction sufficient for the beam design. Supposing the extension model of the stress distribution across the section, the elastic plastic behaviour of the poplar beam reinforced by thin bamboo layers (5 mm thick) was theoretically described. Then the deflection progress was computed according to the model, and compared with the actual data from the experiments on the small scale sandwich beams.

ASSUMPTIONS FOR THE THEORETICAL COMPUTATION

For the appropriate simplification of the theoretical interpretation about the elastic plastic behaviour of the sandwich beam, the following assumptions can be introduced:

1. The modulus of elasticity must be the same in both tension and compression.
2. The section remains plane before and after bending.
3. The materials comprising the beam behave as the perfect elastic plastic body (Fig. 1). The stress–strain relationship of the materials is perfectly elastic until the maximal strength is attained; then the constant plastic flow starts, only in the case of compression loading, while keeping the same stress level. In case of tensile stress the material shows brittle failure at its strength value.
4. The deformation must be kept small.

The validity of these assumptions is widely recognized by experiences and generalized for the plastic design method.

COMPUTATION OF LOADING CAPACITY

Considering the extension of the plastic area resulted from the increasing load, the evolution of the stress distribution across a cross section of the sandwich beam can

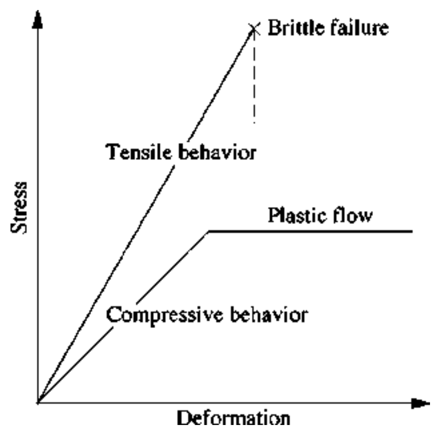

Figure 1. Supposition of material behaviour.

be simplified by the above mentioned assumptions, and the following progressive model, from Step 1 to Step 4, can be proposed.

Step 1 : The cross section is entirely elastic. This state is valid from the beginning of loading until the upper border of the poplar section turns plastic. Since the compressive strength of poplar ($\sigma_{pc.max} \approx 28$ N/mm^2) is much less than that of bamboo ($\sigma_{bc.max} \approx 78$ N/mm^2) and the bamboo layers are supposed relatively thin (5 mm), the upper border of poplar is assumed to turn plastic before the bamboo section.

Step 2 : A part of poplar section within the distance y_p from the upper border turns plastic. This area constantly keeps the maximal compressive strength ($\sigma_{pc.max} \approx 28$ N/mm^2) after yield. The neutral plane starts to move downward.

Step 3 : The plastic area extends from the compressed poplar section to the upper bamboo layer. The plastic area in bamboo is within the distance y_b from the top of bamboo, keeping the maximal stress ($\sigma_{bc.max} \approx 78$ N/mm^2).

Step 4 : The upper layer of bamboo is entirely yielded. The plastic area continues to extend in the compressed poplar area until the external tensile stress in the lower bamboo layer reaches its strength value ($\sigma_{bt.max} \approx 176$ N/mm^2). This tensile failure of bamboo layer provokes the bending failure of the beam.

Even if the tensile strength of poplar ($\sigma_{pt.max} \approx 70$ N/mm^2) is reached before the tensile failure of bamboo, the bamboo layers prevent the failure of the poplar fibre. In this simplified model, it may safely be assumed that tensile stress of poplar continues to rise keeping the elastic distribution, until the tensile failure of the bamboo layers. Although the actual tensile stress distribution remains to be studied, it seems reasonable to apply this supposition for this step in which the mechanical role of poplar is no more important.

Note that the yield stress of each material represents the maximal strength in this description in accordance with the third assumption mentioned above. The maximal strength of each material refers to the published data [2, 3].

Figure 2 illustrates this idealized stress distribution model evolving gradually from Step 1 to Step 4. The MOE of both the top and bottom layers are assumed to be identical in this model. The assumption of the failure in Fig. 2 corresponds to the picture in Fig. 3 presenting the real failure of a bamboo-poplar sandwich beam. In this picture, the compressed poplar fibres show wrinkles as plastic flow. The tensile breaking of bamboo fibres caused the entire failure of the beam.

Taking the example of Step 3, the computation of the theoretical moment M_t is explained below in detail. The other cases, Steps 1, 2 and 4, can be explained similarly.

The relationships of the variables, σ_{bt}, σ_{pt}, y_{np}, y_b and y_p, can be given by the above assumptions. The first assumption gives the linear relationship between the

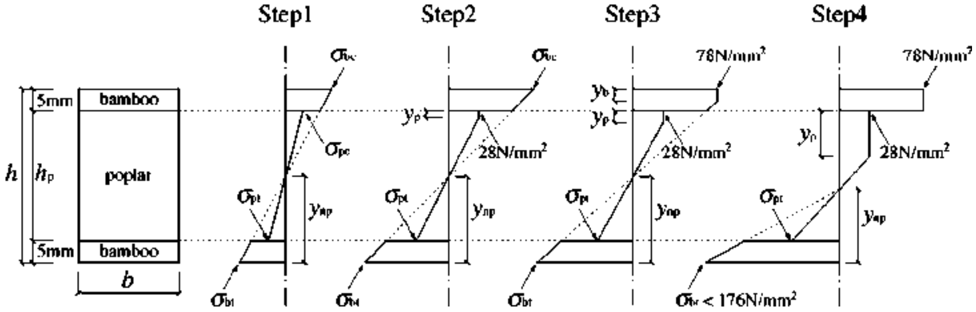

Figure 2. Evolving stress distribution model.

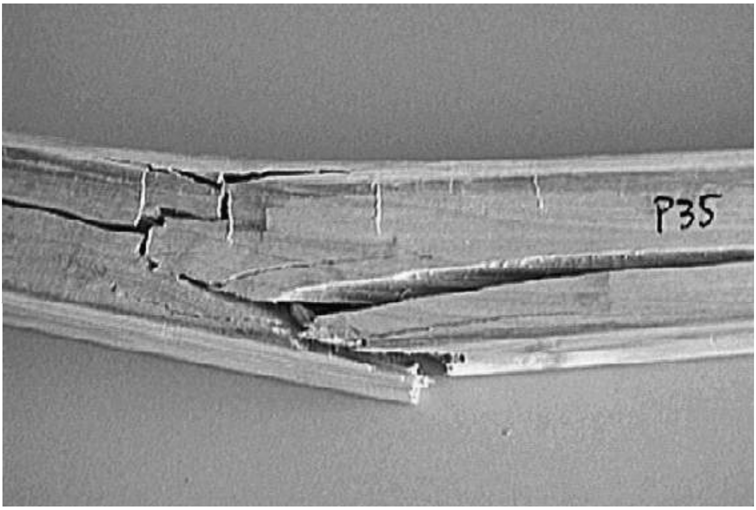

Figure 3. Failure of a bamboo-poplar sandwich beam by four point bending test. This picture shows the centre of the sandwich beam where the rupture took place.

stress and the distance from the neutral plane:

$$\frac{\sigma_{\mathrm{pt}}}{y_{\mathrm{np}} - h_{\mathrm{b}}} = \frac{\sigma_{\mathrm{pc.max}}}{h - h_{\mathrm{b}} - y_{\mathrm{np}} - y_{\mathrm{p}}}, \tag{1}$$

$$\frac{\sigma_{\mathrm{bt}}}{y_{\mathrm{np}}} = \frac{\sigma_{\mathrm{bc.max}}}{h - y_{\mathrm{np}} - y_{\mathrm{b}}}, \tag{2}$$

where the thickness of bamboo layers $h_{\mathrm{b}} = 5$ mm.

According to the second assumption, the distribution of the strain is linear and proportional to the distance from the neutral plane. There is no gap by the deformation at the bonding joints. The longitudinal deformation of poplar is equal to that of bamboo at each joint.

The longitudinal contraction at the upper joint u_1:

$$u_1 = \frac{h - y_{\mathrm{np}} - 5}{y_{\mathrm{np}}} \frac{\sigma_{\mathrm{bt}}}{E_1} = \frac{h - y_{\mathrm{np}} - 5}{h - y_{\mathrm{np}} - y_{\mathrm{p}} - 5} \frac{28}{E_2}, \tag{3}$$

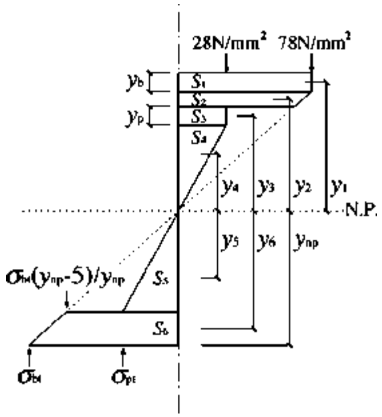

Figure 4. Stress distribution model during Step 3.

in which E_1 is the E of the bamboo and E_2 is the E of the internal material. The longitudinal expansion at the lower joint u_2:

$$u_2 = \frac{\sigma_{pt}}{E_2} = \frac{y_{np} - 5}{y_{np}} \frac{\sigma_{bt}}{E_1}, \tag{4}$$

where E_1 and E_2 are the longitudinal modulus of elasticity of bamboo and that of poplar respectively.

On this model, the moment causing the above stress distributed across the cross section is defined by (see also Fig. 4 for the origin of the axis):

$$M_t = b \int \sigma y \, dy. \tag{5}$$

Equation (5) can be written for Step 3 in the following concrete form:

$$M_t = b \sum S_i y_i = b(S_1 y_1 + S_2 y_2 + S_3 y_3 + S_4 y_4 + S_5 y_5 + S_6 y_6), \tag{6}$$

where y_i is the vertical distance from the neutral plane to the central axis of the ith surface S_i (Fig. 4).

In order to obtain the theoretical moment M_t, as well as the other unknown variables, the position of the neutral plane must be computed. The neutral plane is positioned to realize the equilibrium between the sum of the compressive stress and that of the tensile stress:

$$\sum \sigma_{comp} = \sum \sigma_{tensile}, \tag{7}$$

where

$$\sum \sigma_{comp} = b\left[78 y_b + \frac{1}{2}(5 - y_b)\left(78 + \frac{h - y_{np} - 5}{y_{np}} \sigma_{bt}\right) + 28 y_p + \frac{28}{2}(h - y_{np} - y_p - 5)\right], \tag{8}$$

$$\sum \sigma_{\text{tensile}} = b\left[\frac{1}{2}\sigma_{\text{pt}}(y_{\text{np}} - 5) + \frac{5}{2}\left(\sigma_{\text{bt}} + \sigma_{\text{bt}}\frac{y_{\text{np}} - 5}{y_{\text{np}}}\right)\right]. \tag{9}$$

From equations (1–4),

$$\sigma_{\text{bt}} = 28\frac{E_1}{E_2}\frac{y_{\text{np}}}{h - y_{\text{np}} - y_{\text{p}} - 5}, \tag{10}$$

$$\sigma_{\text{pt}} = 28\frac{y_{\text{np}} - 5}{h - y_{\text{np}} - y_{\text{p}} - 5}, \tag{11}$$

$$y_{\text{b}} = h\left(1 - \frac{78E_2}{28E_1}\right) - y_{\text{np}}\left(1 - \frac{78E_2}{28E_1}\right) + y_{\text{p}}\frac{78E_2}{28E_1} + 5\frac{78E_2}{28E_1}. \tag{12}$$

Substituting σ_{bt}, σ_{pt} and y_{b} into equations (8) and (9), the position of neutral plane y_{np} is written by the equation in term of one variable y_{p}.

Consequently, the neutral plane positions of Steps 1 to 4 can be computed as:

$$\text{Step 1: } y_{\text{np}} = \frac{h}{2}, \tag{13}$$

$$\text{Step 2: } y_{\text{np}} = \frac{1}{2}\left(h - \frac{y_{\text{p}}^2}{h + 10n - 10}\right), \tag{14}$$

$$\text{Step 3: } Ay_{\text{np}}^2 + By_{\text{np}} + C = 0, \tag{15}$$

$$\text{Step 4: } y_{\text{np}} = \frac{7h^2 - 7y_{\text{p}}^2 + 125h - 195y_{\text{p}} + 175n - 975}{14h + 70n + 55}, \tag{16}$$

where $A = -(28n - 78)^2$, $B = 2 \cdot 78(28n - 78)y_{\text{p}} + 2h\{(28n - 78)^2 - 28^2n\} - 20\{(28n - 39)(28n - 78) + 50 \cdot 28n\}$, $C = -(28^2n - 78^2)y_{\text{p}}^2 - 2 \cdot 78\{h(28n - 78) + 5 \cdot 78\}y_{\text{p}} - h^2\{(28n - 78)^2 - 28^2n\} + 10h\{(28n - 78)^2 + 50 \cdot 28n\} - 25 \cdot 78^2$, $n = E_1/E_2$. All the variables necessary to determine the theoretical moment M_{t} can be expressed by one variable y_{p}.

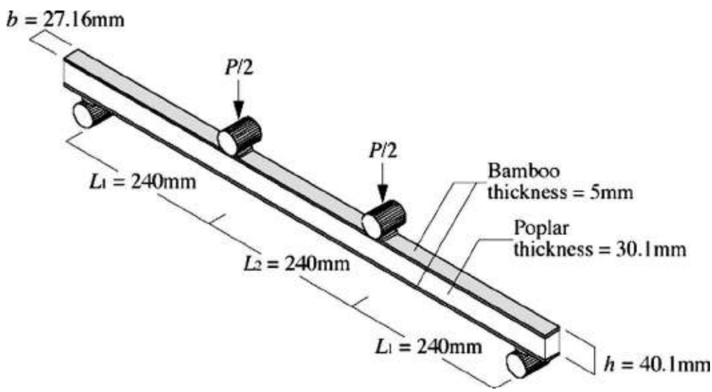

Figure 5. Configuration of the tested beams. Five beams were tested in accordance with a standard four-point bending test method. The dimensions in the figure are the mean values of five specimens.

Table 1 summarizes the results of the computation of the central moment M_t on a type of four point bended sandwich beam (Fig. 5) by the above method. The geometrical parameters (h, b, L_1, L_2) and the modulus of elasticity (E_1, E_2) necessary for the computation of the theoretical moment are obtained as the mean values of the actually tested specimens.

$$h = 40.1 \text{ mm}, \quad b = 27.16 \text{ mm}, \quad L_1 = L_2 = 240 \text{ mm},$$
$$n = \frac{E_1}{E_2} = \frac{10821}{8346} \approx 1.3.$$

The dimensions of the specimens, relatively small, were decided in accordance with the size of the available materials.

In the case of this beam, the above computation concludes that the elastic limit and the maximal loading capacity are given by the moment of 318.5 N mm and of 694.2 N mm, respectively.

COMPUTATION OF DEFLECTION

Following the computation of the theoretical moment, the instantaneous deflection of the beam evolving from the application of load until its rupture is calculated in this paragraph. The results of computations give the theoretical load–deflection curve that can provide more detailed information comparable with the actual curves. As for the distribution of the moment along a beam in the four-point bending test, the moment in the central span between the two loaded points is constant, while the outer spans have the linear diminution of the moment from the loaded points to the supporting points. Applying the second assumption, the section plane before bending remains plane after bending. The radius of curvature ρ of the deflection is given by

$$\rho = \frac{E}{\sigma_{\mathrm{bt}}} y_{\mathrm{np}}. \tag{17}$$

Equation (17) gives the constant curvature along the span under the constant moment, and gradient curvature in the outer spans.

In order to obtain the central deflection of the beam in the range of the above assumption, the gradient moment distribution is simplified to stepwise distribution. The pure bending deflection between the supporting points and the loaded points can be assumed to be the sum of the deflections of the small fragments $\Sigma\delta$ (Fig. 6). The curvature of each fragment is constant.

The actual deflection δ_{total} of the four point loaded beam with rectangular cross section beam in Fig. 6 consists of the above-stated pure bending deflection and the shearing deformation:

$$\delta_{\mathrm{total}} = \sum_{i=0}^{n} \delta_i + \frac{f}{GA}\left(\frac{P}{2}\right)\frac{L}{3} = \sum_{i=0}^{n} \delta_i + \frac{PL}{5GA}, \tag{18}$$

where the form factor of the rectangular cross section $f = 6/5$.

Table 1.
Computation results of the theoretical moment M_t at the central span of a four point loaded beam

Beam type		h 40.1 mm	h_p 30.1 mm	b 27.16 mm	L_1 (= L_2) 240 mm	n ($\approx E_1/E_2$) 1.3		
	Plastic area		Neutral plane	Extreme stress of bamboo		Extreme stress of poplar		Theoretical moment
	In poplar	In bamboo		Tension	Compression	Tension	Compression	
	y_p (mm)	y_b (mm)	y_{np} (mm)	σ_{bt} (N/mm^2)	σ_{bc} (N/mm^2)	σ_{pt} (N/mm^2)	σ_{pc} (N/mm^2)	M_t (kN mm)
Step 1	0.00	0.00	20.05	0.00	0.00	0.00	0.00	0.00
	0.00	0.00	20.05	48.49	48.49	28.00	**28.00**	318.53
Step 2	0.50	0.00	20.05	50.14	50.16	28.95	**28.00**	329.31
	1.00	0.00	20.04	51.87	51.93	29.95	**28.00**	340.52
	1.50	0.00	20.02	53.69	53.83	30.99	**28.00**	352.19
	2.00	0.00	20.00	55.60	55.86	32.08	**28.00**	364.37
	2.50	0.00	19.98	57.61	58.03	33.22	**28.00**	377.11
	3.00	0.00	19.95	59.73	60.36	34.43	**28.00**	390.46
	3.50	0.00	19.91	61.98	62.86	35.70	**28.00**	404.47
	4.00	0.00	19.86	64.35	65.56	37.04	**28.00**	419.24
	5.91	0.00	19.64	74.91	**78.00**	42.96	**28.00**	484.00
Step 3	6.00	0.18	19.63	75.47	**78.00**	43.27	**28.00**	487.41
	6.5	1.15	19.54	78.51	**78.00**	44.94	**28.00**	504.87
	7.00	2.08	19.42	81.39	**78.00**	46.49	**28.00**	520.03
	7.50	2.97	19.26	84.12	**78.00**	47.91	**28.00**	532.89
	8.00	3.84	19.09	86.68	**78.00**	49.21	**28.00**	543.45
	8.50	4.68	18.88	89.05	**78.00**	50.36	**28.00**	551.69
	8.70	5.00	18.80	89.92	**78.00**	50.77	**28.00**	554.27

Table 1.
Computation results of the theoretical moment M_t at the central span of a four point loaded beam

Beam type		h	h_p	b	$L_1\ (= L_2)$	$n\ (\approx E_1/E_2)$		
		40.1 mm	30.1 mm	27.16 mm	240 mm	1.3		
	Plastic area		Neutral plane	Extreme stress of bamboo		Extreme stress of poplar		Theoretical moment
	In poplar	In bamboo		Tension	Compression	Tension	Compression	
	y_p (mm)	y_b (mm)	y_{np} (mm)	σ_{bt} (N/mm^2)	σ_{bc} (N/mm^2)	σ_{pt} (N/mm^2)	σ_{pc} (N/mm^2)	M_t (kN mm)
Step 4	9.00	5.00	18.66	91.27	**78.00**	51.39	**28.00**	558.03
	10.50	5.00	17.96	98.37	**78.00**	54.60	**28.00**	576.48
	12.00	5.00	17.21	106.31	**78.00**	58.02	**28.00**	594.85
	13.50	5.00	16.42	115.27	**78.00**	61.66	**28.00**	613.13
	15.00	5.00	15.58	125.46	**78.00**	65.53	**28.00**	631.31
	16.50	5.00	14.70	137.14	**78.00**	69.61	**28.00**	649.37
	18.00	5.00	13.77	150.69	**78.00**	73.84	**28.00**	667.29
	19.50	5.00	12.80	166.62	**78.00**	78.11	**28.00**	689.05
	20.28	5.00	12.28	176.00	**78.00**	80.28	**28.00**	694.15

For all beam types $h = 40.1$ mm, $h_p = 30.1$ mm, $b = 27.16$ mm, $L_1 (= L_2) = 240$ mm, $n(\approx E_1/E_2) = 1.3$.

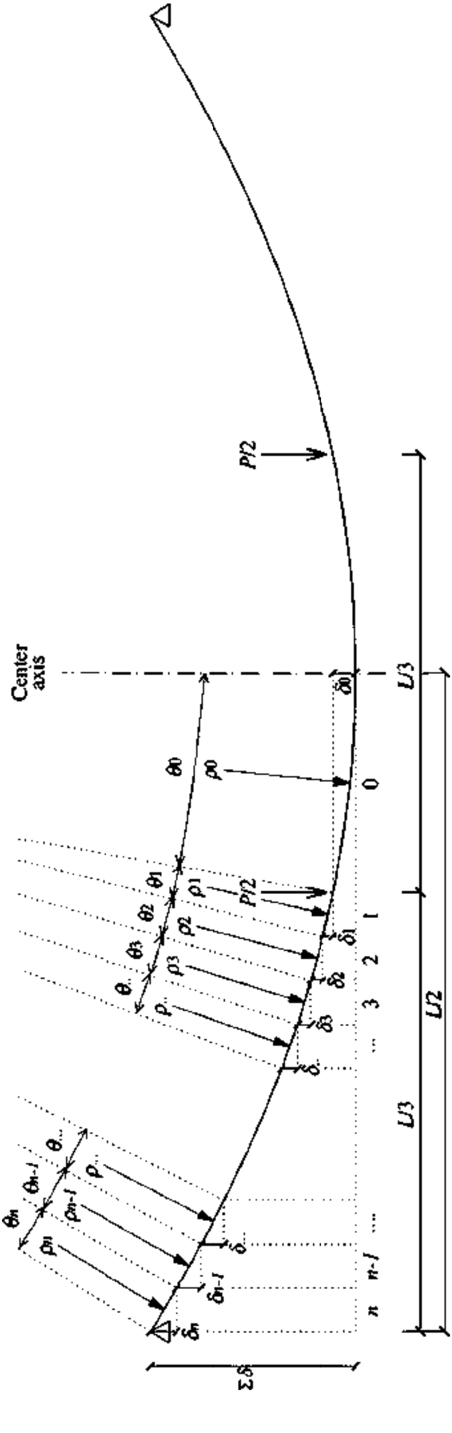

Figure 6. Fragmented deflection of the four point loaded beam.

The first term of the right-hand side, meaning the pure bending deflection, is given by

$$\sum_{i=0}^{n}\delta_i = \delta_0 + \sum_{i=1}^{n}\delta_i = \rho_0(1-\cos\theta_0) + \sum_{i=1}^{n}\rho_i\left(\cos\sum_{j=0}^{i-1}\theta_j - \cos\sum_{j=0}^{i}\theta_j\right). \quad (19)$$

Hence

$$\delta_{\text{total}} = \rho_0(1-\cos\theta_0) + \sum_{i=1}^{n}\rho_i\left(\cos\sum_{j=0}^{i-1}\theta_j - \cos\sum_{j=0}^{i}\theta_j\right) + \frac{PL}{5GA}, \quad (20)$$

where

$$\theta_0 = \sin^{-1}\left(\frac{L}{6\rho_0}\right), \quad \sum_{j=0}^{i}\theta_j = \sin^{-1}\left(\frac{L}{3n}\sum_{j=1}^{i}\frac{1}{\rho_j} + \frac{L}{6\rho_0}\right). \quad (21)$$

Substituting equation (21) into equation (20), the central deflection of the four point loaded beam can be written in terms of the radius of curvature ρ. Assuming that ρ is given by equation (17), the central deflection can be computed with the extreme stress of bamboo σ_{bt} and the neutral plane position y_{np}. These variables are already obtained in the previous paragraph. For the example of computing the deflection of the beam, the outer spans between loaded points and the supporting points were divided into twelve fragments ($n = 12$). The length of each fragment was 20 mm.

The values in the left column in Table 2 are the central moment M_0 of the four point loaded beam evolving with the load increase. These are equal to the theoretical moment M_{t} calculated in Table 1. The value M_i means the moment of the ith fragment of the beam. The radius of curvature ρ_i results from equation (17), in which the value for σ_{bt} is computed depending on M_i. The values for ρ_i, σ_{bt} and M_i are defined by the following procedure. For example, when the cross-section of the top bamboo layer is entirely turned into plastic, the central moment M_0 takes the value of 554 N mm in Step 3. On this beam, the moment at the cross section at 50 mm from the loaded points toward the nearer supporting point is

$$M_3 = 554\left(\frac{L}{3} - 50\right)\Big/\left(\frac{L}{3}\right) \approx 439 \text{ N mm}.$$

The cross section, taking the moment 439 N mm, is in the state of Step 2. Referring to equations (6), (10) and (14), the variables σ_{bt} and y_{np} are given as

$$\sigma_{\text{bt}} = 67.524 \text{ N/mm}^2, \quad y_{\text{np}} = 19.802 \text{ mm}.$$

Substituting the values into equation (17), the radius of curvature ρ_3 is

$$\rho_3 = \frac{E}{\sigma_{\text{bt}}}y_{\text{np}} = \frac{10821}{67.524} \times 19.802 \approx 3173 \text{ mm}.$$

Table 2.
Computation results of the curvature of the deflection ρ depending on the bending moment M

	Distance from the loaded points (mm)																									
	0		10		30		50		70		90		110		130		150		170		190		210		230	
	M_0	ρ_0	M_1	ρ_1	M_2	ρ_2	M_3	ρ_3	M_4	ρ_4	M_5	ρ_5	M_6	ρ_6	M_7	ρ_7	M_8	ρ_8	M_9	ρ_9	M_{10}	ρ_{10}	M_{11}	ρ_{11}	M_{12}	ρ_{12}
Step 1	0		0		0		0		0		0		0		0		0		0		0		0		0	
	319	4474	305	4669	279	5113	252	5651	226	6316	199	7159	173	8260	146	9762	119	11931	93	15340	66	21476	40	35793	13	107378
Step 2	329	4326	316	4516	288	4946	261	5466	233	6110	206	6924	178	7989	151	9442	123	11540	96	14837	69	20772	41	34621	14	103862
	341	4180	326	4366	298	4783	270	5286	241	5908	213	6696	184	7726	156	9131	128	11160	99	14349	71	20089	43	33481	14	100443
	352	4036	338	4219	308	4624	279	5111	249	5713	220	6474	191	7470	161	8829	132	10790	103	13873	73	19423	44	32371	15	97114
	364	3893	349	4072	319	4470	288	4940	258	5522	228	6258	197	7221	167	8533	137	10430	106	13410	76	18774	46	31289	15	93868
	377	3752	361	3927	330	4317	299	4774	267	5335	236	6046	204	6977	173	8245	141	10077	110	12957	79	18139	47	30232	16	90697
	390	3613	374	3784	342	4166	309	4610	277	5153	244	5840	211	6738	179	7963	146	9733	114	12514	81	17519	49	29199	16	87597
	404	3476	388	3642	354	4015	320	4451	287	4974	253	5637	219	6505	185	7687	152	9396	118	12080	84	16912	51	28187	17	84561
	419	3340	402	3502	367	3865	332	4292	297	4799	262	5439	227	6276	192	7417	157	9065	122	11655	87	16317	52	27194	17	81583
	484	2838	464	2980	424	3303	383	3688	343	4151	303	4711	262	5436	222	6424	182	7852	141	10095	101	14133	61	23555	20	70666
Step 3	487	2815	467	2956	426	3277	386	3660	345	4121	305	4678	264	5398	223	6379	183	7797	142	10025	102	14034	61	23391	20	70172
	505	2693	484	2839	442	3149	400	3522	358	3971	316	4516	273	5211	231	6159	189	7527	147	9678	105	13549	63	22582	21	67745
	520	2581	498	2739	455	3045	412	3408	368	3848	325	4384	282	5059	238	5979	195	7308	152	9396	108	13154	65	21924	22	65771
	533	2478	511	2651	466	2962	422	3317	377	3749	333	4277	289	4937	244	5835	200	7131	155	9169	111	12837	67	21394	22	64183
	543	2383	521	2575	476	2896	430	3245	385	3670	340	4191	294	4841	249	5721	204	6993	159	8991	113	12587	68	20979	23	62936
	552	2295	529	2513	483	2846	437	3190	391	3610	345	4126	299	4769	253	5636	207	6889	161	8857	115	12399	69	20666	23	61997
	554	2262	531	2492	485	2831	439	3173	393	3592	346	4106	300	4747	254	5610	208	6856	162	8815	115	12341	69	20569	23	61707
Step 4	558	2212	535	2462	488	2809	442	3149	395	3565	349	4077	302	4715	256	5572	209	6810	163	8756	116	12258	70	20431	23	61292
	576	1975	552	2285	504	2697	456	3035	408	3439	360	3940	312	4564	264	5394	216	6592	168	8476	120	11866	72	19777	24	59330
	595	1752	570	2056	520	2578	471	2928	421	3321	372	3810	322	4423	273	5227	223	6389	173	8214	124	11500	74	19166	25	57498
	613	1541	588	1839	536	2447	485	2828	434	3210	383	3688	332	4289	281	5071	230	6198	179	7969	128	11157	77	18595	26	55784
	631	1344	605	1633	552	2286	500	2729	447	3106	395	3572	342	4162	289	4925	237	6020	184	7740	132	10835	79	18059	26	54177
	649	1160	622	1440	568	2080	514	2626	460	3008	406	3463	352	4041	298	4788	244	5852	189	7524	135	10534	81	17557	27	52670
	667	989	639	1259	584	1884	528	2516	473	2916	417	3360	361	3927	306	4660	250	5695	195	7322	139	10251	83	17085	28	51256
	685	832	657	1090	599	1698	5429	2393	485	2829	428	3632	371	3818	314	4539	257	5548	200	7133	143	9986	86	16643	29	49928
	694	755	665	1008	607	1606	550	2319	492	2785	434	3214	376	3764	318	4479	260	5475	202	7039	145	9855	87	16424	29	49273

Units: M_i (kN mm), ρ_i (mm).

Table 3.
Computation results of the theoretical deflection

	Theoretical maximal moment $M_t = M_0$ (kN mm)	Bending deflection δ_b (mm)	Shearing deformation δ_s (mm)	Total deflection δ_{total} (mm)
Step 1	0	0.00	0.00	0.00
	319	10.73	0.75	11.48
Step 2	329	11.10	0.77	11.87
	341	11.48	0.80	12.28
	352	11.89	0.83	12.72
	364	12.32	0.85	13.17
	377	12.77	0.88	13.66
	390	13.25	0.92	14.17
	404	13.77	0.95	14.71
	419	14.31	0.98	15.29
	484	16.78	1.13	17.92
Step 3	487	16.92	1.14	18.06
	505	17.64	1.18	18.83
	520	18.34	1.22	19.56
	533	19.01	1.25	20.26
	543	19.65	1.27	20.93
	552	20.26	1.29	21.56
	554	20.49	1.30	21.79
Step 4	558	20.85	1.31	22.16
	576	22.80	1.35	24.15
	595	25.15	1.39	26.54
	613	27.95	1.44	29.39
	631	31.37	1.48	32.85
	649	35.62	1.52	37.14
	665	40.81	1.56	42.37
	681	47.53	1.60	49.12
	689	51.82	1.62	53.44

The same process of computation can obtain all the values in Table 2. Substitution of these values into equations (20) and (21) attains the estimation of the deflection. The results are presented in Table 3.

So as to overestimate the shearing deformation of the beam, the deformation of the thin bamboo layers was neglected. Though the shearing stress is propagated into the bamboo layers, the bamboo cross section area was eliminated from the concerned area.

$$A = A_{\text{poplar}}.$$

The modulus of rigidity of the beam is considered equal to that of poplar. The value is approximately estimated regarding the MOE of poplar [4]:

$$G \approx 0.075\text{MoE}_{\text{poplar}} = 0.075 \times 8346.4 \approx 626\ \text{N/mm}^2.$$

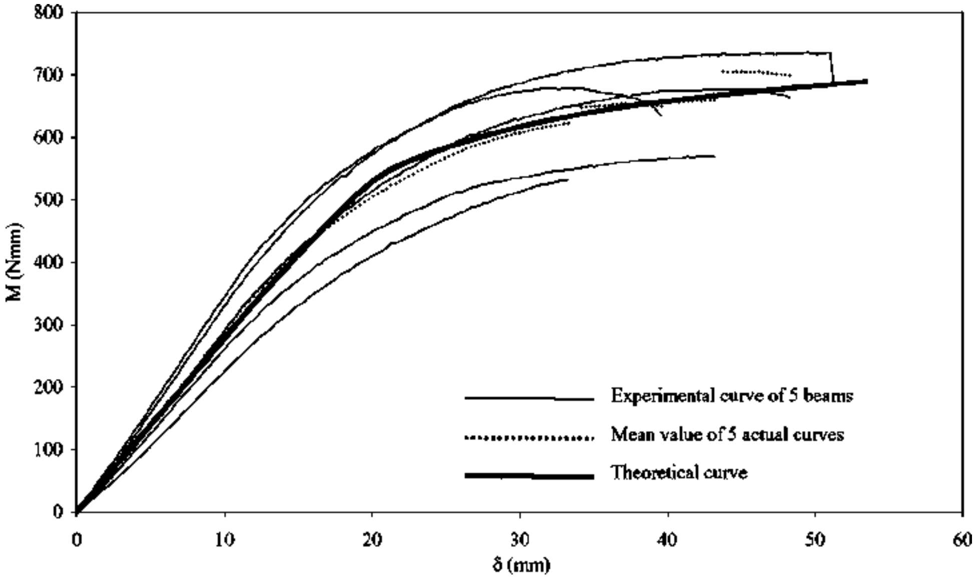

Figure 7. Comparison between the theoretical moment–deflection curve and the actual curves. The fine curves represent the bending behaviour of the five tested beams, while the bold dotted curve is their mean values. The bold curve, the result of theoretical computation, is superposed on these experimental results.

The estimated shearing deformation of the beam is small enough to be neglected.

ADEQUACY OF THE THEORETICAL COMPUTATION METHOD TO THE PREDICTION OF THE BENDING BEHAVIOUR

The content of Table 3 is illustrated in Fig. 7, and compared with the actual data from the experiments. The bold curve traces the moment-deflection correlation given by the previous Table 3, resulted from the computation of this paragraph, while the fine curves trace the experimental data of the five beams. The test method and the disposition of these beams follow Fig. 5. The theoretical estimation and the actual data show an interesting similarity. The efficiency of the theoretical estimation is presented more clearly by the comparison with the mean value of the five beams. The bold-dotted line in Fig. 7 traces the mean value of the actual curves in Fig. 7. Not only the ultimate strength, but also the elastic plastic evolution of bending capacity can be estimated with enough precision by the theoretical computation.

CONCLUSIONS

As for the prediction of the bending strength, a model extending its plastic area across the section was studied. The moment–deflection curve was then computed on the basis of this stress distribution model. The correspondence of this theoretical curve to the actual curves, given by the tests on the five small sandwich beams, was remarkably well. This computation can be considered effective to estimate the ultimate strength of the sandwich beam as well as the elastic plastic deflection evolution.

Acknowledgements

This research project was supported by Prof. J. Natterer, Swiss Federal Institute of Technology, Prof. M. Ohta, University of Tokyo and the Swiss National Science Foundation.

REFERENCES

1. Y. Amino, Conception and feasibility of bamboo — precocious wood composite beams, *Journal of Bamboo and Rattan* **2** (3), 261–279 (2003).
2. R. Shikenjo, *Mokuzai Kogyo Handbook.* Maruzen, Tokyo (1982) (in Japanese).
3. J. Sell and F. Kropf, *Propriété et Caractéristiques des Essences de Bois.* Lignum, Zurich (1989).
4. Forest Products Laboratory, *Wood Handbook: Wood as an Engineering Material.* US Department of Agriculture, Washington, DC (1987).